Anchorage of naturally corroded bars in reinforced concrete structures

Mohammad Tahershamsi
MSc-Doctoral candidate, Department of Civil and Environmental Engineering, Division of Structural Engineering, Concrete Structures, Chalmers University of Technology, Gothenburg, Sweden

Kamyab Zandi
PhD Researcher, Materials Group, CBI Swedish Cement and Concrete Research Institute, Borås, Sweden; Research Assistant, Department of Civil and Environmental Engineering, Division of Structural Engineering, Concrete Structures, Chalmers University of Technology, Gothenburg, Sweden

Karin Lundgren
Professor, Department of Civil and Environmental Engineering, Division of Structural Engineering, Concrete Structures, Chalmers University of Technology, Gothenburg, Sweden

Mario Plos
Associate Professor, Department of Civil and Environmental Engineering, Division of Structural Engineering, Concrete Structures, Chalmers University of Technology, Gothenburg, Sweden

The bond properties of naturally corroded reinforced concrete members were experimentally investigated. Thirteen specimens were taken from the northern edge beam of Stallbacka Bridge, a girder bridge in Sweden. The specimens exhibited different levels of corrosion-induced damage, including concrete cracking and cover spalling. The damage was carefully documented and the specimens were tested in suspended four-point bending tests. Their general behaviour was monitored through measurements of applied loads and vertical deflections. At the same time, the local anchorage behaviour was recorded at the end regions. The test results showed around 5% lower anchorage capacity for damaged specimens compared with the reference ones. The residual bond strength was studied with respect to the observed damage. These tests, and artificial corrosion results from the literature, indicate that the bond strength decreased with increasing maximum splitting crack widths. However, the bond capacity was higher for the naturally corroded specimens. The results thus show an obvious difference between artificial and natural corrosion, and furthermore indicate that the provisions given in fib Model Code 2010 are on the safe side. These test results contribute to further knowledge regarding the structural behaviour of corroded reinforced concrete structures.

Notation

d effective cross-sectional height
F_t estimated tensile force in tensile bars
f_c compressive strength of cylindrical concrete specimen
l_a available anchorage length
l_s shear span length
P applied single load from load cell
ϕ main bar diameter

Introduction

Deterioration caused by aggressive agents is a very common, serious and costly problem in existing concrete structures. Almost all types of structural concrete contain steel in the form of reinforcements or tendons or a combination of both. Corrosion of these steel components leads to several undesirable effects in a concrete member. One possible severe damage state is a loss in steel cross-sectional area, which reduces both the capacity and the ductility of the reinforcement (Almusallam, 2001; Du et al., 2005a, 2005b). Corrosion of embedded steel reinforcement also damages the surrounding concrete. Corrosion products occupy a much higher volume than the original steel, which increases the pressure around the reinforcement. This results in concrete crack-

ing, cover spalling and degradation of reinforcement–concrete bond properties (Al-Sulaimani et al., 1990). Such defects occurring in the anchorage zones of load-carrying members can significantly affect the mechanical performance of a structure (Regan and Kennedy Reid, 2010; Zandi Hanjari et al., 2011a). Loss of ductility and stiffness during the service life (Coronelli and Gambarova, 2004; Zandi Hanjari et al., 2011b) and a decrease in load-carrying capacity in the ultimate limit state (Val et al., 2009) are among the main structural issues observed in cases of corrosion damage.

Numerous studies have investigated the parameters that may influence the bond and anchorage capacity of corroded reinforced concrete (for the latest findings see work by Coronelli et al. (2013), Regan and Kennedy Reid (2010), Sæther (2011) and Zandi Hanjari et al. (2011b)). However, existing knowledge is mostly based on experimental investigations of specimens that have been subjected to accelerated corrosion, for example by application of impressed current density. The current densities applied in laboratory work usually vary in the range 0·05–5·00 mA/cm², which is noticeably higher than natural values measured in the field, and deterioration caused by artificial

Magazine of Concrete Research
Volume 66 Issue 14

Anchorage of naturally corroded bars in
reinforced concrete structures
Tahershamsi, Zandi, Lundgren and Plos

corrosion may affect the structural behaviour in different ways compared with natural corrosion.

Experimental evidence reported in the literature shows that common methods of accelerated induced corrosion may influence the bond capacity and change the anchorage behaviour (Austin *et al.*, 2004; Saifullah and Clark, 1994). Yuan *et al.* (2007) found that the corroded steel surface morphology was homogeneous in accelerated corrosion tests while, in natural corrosion conditions, the steel surface corroded heterogeneously. Furthermore, the longer time span required for natural corrosion means that time-dependent effects (e.g. shrinkage, creep and the transport of corrosion products through cracks) will differ. Furthermore, in many countries, freezing will affect the natural behaviour. Nevertheless, the strong justification for using accelerated induced corrosion in laboratory tests is the reduction of corrosion time from several decades to a few weeks. To better correspond to reality, it has been suggested that artificial corrosion tests should be carried out using relatively low current densities, such as 0.05 mA/cm^2 (Coronelli, 1997), and that the results should be interpreted and extrapolated to field practice with great care. There is thus a strong requirement for experiments on natural corrosion to facilitate evaluation of the accelerated corrosion tests available in the literature.

As the process of natural corrosion takes several years, corroded specimens from existing structures were collected. In two series of tests, the anchorage capacity of naturally corroded steel bars embedded in concrete was investigated. In the first test series, eight specimens with different degrees of corrosion damage were taken from the southern edge beam of the concrete deck of Stallbacka Bridge. An appropriate test setup was designed (Berg and Johansson, 2011) and the specimens were tested successfully. The results of the first test series showed almost 10% lower load-carrying capacity for the corroded specimens than for undamaged ones (Lundgren *et al.*, 2014; Tahershamsi *et al.*, 2012a, 2012b).

The results of the second series of experiments are presented and analysed in this paper. Thirteen specimens were taken from the northern edge beam of Stallbacka Bridge and tested in a similar four-point bending test configuration, indirectly supported by suspension hangers, as in the first test series. The corrosion process had taken place naturally over approximately 30 years of the bridge service life. The anchorage behaviour of the reinforcement was investigated through measurements of the applied load, free-end slip and mid-span deflection. The aim of the experiments was to study the influence of natural corrosion on the mechanical behaviour of damaged concrete members, particularly the anchorage capacity. In this study, an effort was made to understand the correlations between the visually observed corrosion damage and the anchorage capacity and to form a basis for comparison of natural versus accelerated corrosion test data.

Test specimens

The specimens were chosen from the concrete edge beams of a steel girder bridge with a concrete deck slab. The bridge, Stallbacka Bridge, is located in the south-west of Sweden in an aggressive environment due to the use of de-icing salt during the winter. For this reason, corrosion was considered as the main cause of deterioration. Despite the fact that the bridge was built only 30 years ago, it was impaired by the severity of the deterioration and the outermost part of the cantilevering deck and the edge beams were replaced in a rehabilitation project from 2010 to 2012. When constructed, the bridge deck was cast in segments with cast joints in the transversal direction of the bridge, through both bridge slab and the edge beams. The amount of reinforcement across these joints in the slab was insufficient and therefore the edge beams were subjected to more load than they were designed for, leading to the appearance of large cracks. To prevent moisture and snow freezing on the bridge deck, de-icing salt was applied. Chlorides from the de-icing salt reached the steel bars through the load-induced cracks in the concrete. Furthermore, transverse cracks at the construction joints may have accelerated chloride penetration.

The edge beams along the bridge deck showed different amounts of corrosion-induced damage, from no sign of corrosion to extensive cover cracking, resulting in spalling of the concrete cover. This was considered to be an advantage for specimen selection since it was thus possible to acquire specimens with varying levels of damage. Based on the damage patterns, the test specimens were sorted into three groups

- reference (R) specimens without any visible cracks
- specimens with medium damage (M) (spalling cracks)
- specimens with a high degree of damage (H) (cover spalling).

In the first test series, large variations were observed in the capacity of the M specimens. Therefore, in this test series, more specimens of type M were selected.

The geometry of the edge beams was suitable for bending tests, which made it possible to evaluate the anchorage behaviour at a structural level. Figure 1 shows the geometry of the edge beams. The cross-section of the beams was 350×400 mm^2, with a small inclination of the upper surface. Both longitudinal and transversal reinforcements in the edge beams were ribbed. The studied tensile reinforcements were four bars of $\varnothing 16$ Ks60 bundled in pairs, see Table 1. The transverse reinforcement consisted of stirrups $\varnothing 10$ Ks40 with a spacing of 300 mm. Due to differing precision in the construction stage, the concrete cover of the longitudinal reinforcement varied (see Table 2 and Figure 2). No sign of corrosion was observed around the longitudinal reinforcement bars close to the bottom surface of the edge beams. The longitudinal reinforcement bars closest to the upper inclined surface of the edge beams were severely damaged as they were the most exposed to de-icing salt; these were therefore more relevant for investigation of bond and anchorage behaviour.
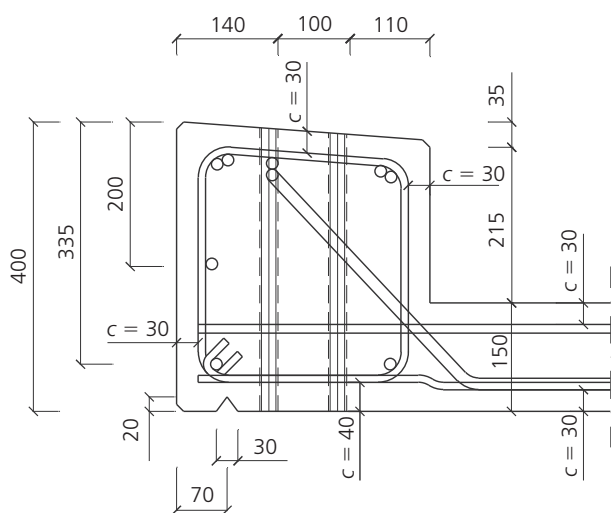
Magazine of Concrete Research
Volume 66 Issue 14

Anchorage of naturally corroded bars in
reinforced concrete structures
Tahershamsi, Zandi, Lundgren and Plos

Figure 1. Cross-sectional details of the edge beam, adapted from
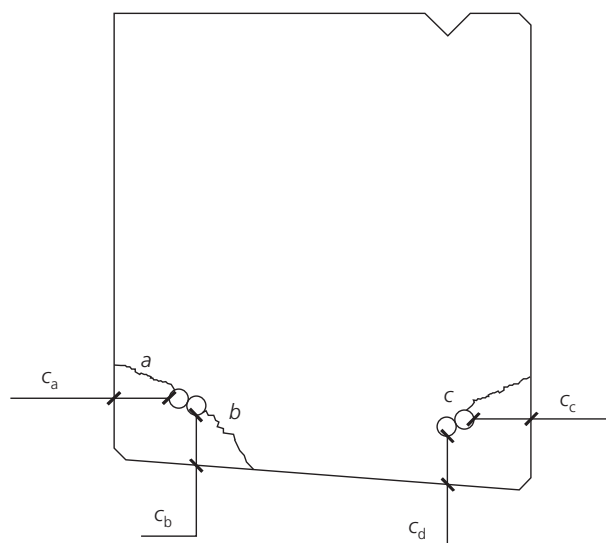bridge drawings. All dimensions are in mm; c is cover thickness

Figure 2. Concrete cover and spalling crack notations; the
orientation of the cross-section in the test rig is also shown

Reinforcement type	Specification
Longitudinal bars (inclined surface)	4 Ø16 Ks60 bundled
Longitudinal bars (levelled surface)	2 Ø16 Ks60
Longitudinal bar (at mid-height)	1 Ø16 Ks60
Stirrups	Ø10 Ks40, spacing 300 mm
Strengthening bars	Ø10 Dywidags

Table 1. Reinforcement details

Specimen	c_a: mm	c_b: mm	c_c: mm	c_d: mm
R4	60	48	45	65
R6	58	57	56	45
M4	70	45	40	65
M5	60	42	46	64
M7	31	74	60	51
M8	45	45	60	40
M9	45	50	55	50
M10	50	55	45	60
M11	62	73	35	69
M12	32	85	62	60
H5	68	30	55	54
H6	72	54	39	60
H7	30	70	65	50

Table 2. Size of concrete covers in the failure region of the tested
specimen

Experimental details

All the beam tests were carried out at the Structural Engineering
Laboratory of Chalmers University of Technology. Based on
experience obtained from the first test series, the measurements
in the tests were slightly modified, as described later in the paper.
Crack and spalling patterns were documented before, during and
after the tests. Material tests were carried out on drilled cores,
and the beams were saved after testing for measurements of the
corrosion level and reinforcement tensile tests.

Material properties

In the second test series, only cores of suspension holes were
drilled out. Drilling of the specimens was performed according to
BS EN 12504-1:2009. Cylindrical cores of 110 mm height and
55 mm diameter were used in compression tests. The tests on
cylindrical compressive strength were performed according to BS
EN 12390-3:2009; the results are given in Table 3. The average
compressive strengths of the H and M specimens were approxi-
mately 85–90% of the strength of the R specimens. It may thus
be concluded that the lower concrete strength could have influ-
enced the damage level.

Experimental setup

The test configuration was designed to secure anchorage failure
for beams with different degrees of corrosion damage in one
common test setup (Berg and Johansson, 2011). A four-point
bending test indirectly supported by suspension hangers was
chosen (Figure 3). Since it was considered important to have the
suspension holes positioned between two stirrups, the holes were
located in advance. In some cases, it was necessary to move the
support hole closer to the centre of the specimen in order not to
drill the outermost stirrups. In such cases, the two support holes
were both moved closer to the centre to maintain symmetry of

Magazine of Concrete Research
Volume 66 Issue 14

Anchorage of naturally corroded bars in
reinforced concrete structures
Tahershamsi, Zandi, Lundgren and Plos

Specimen	f_c: MPa	Average f_c: MPa	Standard deviation: MPa
Reference (R)			
R4-1	48·0		
R4-2	49·2		
R4-3	60·0		
R6-1	54·5		
R6-2	53·0		
R6-3	46·2	51·8	5·1
Medium damage (M)			
M4-1	56·1		
M4-2	45·1		
M5	—		
M7-1	37·5		
M7-2	44·2		
M7-3	42·9		
M7-4	45·8		
M8-1	59·7		
M8-2	48·6		
M8-3	52·7		
M9-1	33·9		
M9-2	50·1		
M9-3	50·6		
M10-1	52·6		
M10-2	40·2		
M11-1	31·8		
M11-2	52·4		
M11-3	48·5		
M12-1	37·9		
M12-2	43·9	46·0	7·5
High damage (H)			
H5-1	50·0		
H6-1	49·2		
H6-2	37·1		
H6-3	39·2		
H7-1	47·9		
H7-2	33·1	42·8	7·2

Table 3. Compressive strength test results of core specimens
taken from the edge beams

the specimens. Thus, the span length between the supports varied
slightly (see Figure 3 and Table 4). However, the shear span was
kept constant and equal to 570 mm.

The edge beams were strengthened by four transverse reinforce-
ments on each side of the suspension holes to avoid premature
failure of the beams in the support regions. Steel bars of
∅20 mm were injected in the drilled cores with epoxy to
strengthen the support region. These strengthening bars were
anchored at the top of the beam using hexagonal nuts and flat
steel plates (Figure 3). The mechanical locking of the bars, by
means of threaded coupling, provided adequate anchorage to

avoid failure at the suspension holes. In the first test series, the
support settlements were measured on top of the flat steel plates,
but these measurements also included the settlements between the
steel plates and the beam. To avoid this problem in the second
series, the steel plates were drilled in certain locations and the
linear variable differential transformers (LVDTs) at the supports
were set on top of the concrete surface.

The load was applied by two symmetrically placed hydraulic
jacks connected to one hydraulic pump to yield equally large
loads. Each of the loads was measured by load cells placed on
the top of each jack. Steel plates and wood-fibre plates were
placed between the hydraulic jacks and the beam; the plates'
dimensions were 100 mm along the beam and 250 mm across the
beam. The tests were conducted by controlling the displacement
in the mid-span. Displacement transducers measured the vertical
displacements relative to the floor in mid-span, in sections of the
suspensions, and at the loads. Furthermore, one displacement
transducer per main bar was placed on the short face of the beam
ends to measure the free-end slip of the longitudinal reinforce-
ment. Two displacement transducers were used to measure the
displacement of the concrete at approximately the same level as
the main bars. These end slips and concrete cross-sectional
displacements were measured relative to a point on the short face
of the beam end, located 185 mm from the top of the beam. All
measurements were continuously stored in a datalogger with an
amplitude of 1 Hz. To avoid unexpected settlements during the
tests, all specimens were loaded up to 35 kN and then unloaded.
Thereafter, loading was applied in steps and the crack develop-
ment was continuously registered up to the failure load.

In summary, modifications of the tests compared to the first test
series were applied mostly to the measurement system. First, the
true support settlements were measured by adjusting the strength-
ening steel plates and placing the displacement transducers on the
top surface of the beams. Second, the displacement of the
concrete close to the main bars was measured to enable more
correct evaluation of the free-end slip; for more information see
Gestsdottir and Gudmundsson (2012).

Results

Documentation of damage before tests

Before the experiments, all visible cracks were marked and
measured. For most of the specimens, the crack widths were first
measured on the bridge. After moving the samples to the
laboratory, the crack widths and spalled concrete covers were
thoroughly documented for a second time, for all specimens.
Comparison of the crack widths from the two measurements, on
the bridge and in the lab, showed minor differences for most
specimens. Some measured crack widths had widened by up to
0·5 mm. However, a few crack widths measured in the lab were
narrower than the values recorded on the bridge. From the
measurements just before structural testing, the crack widths of
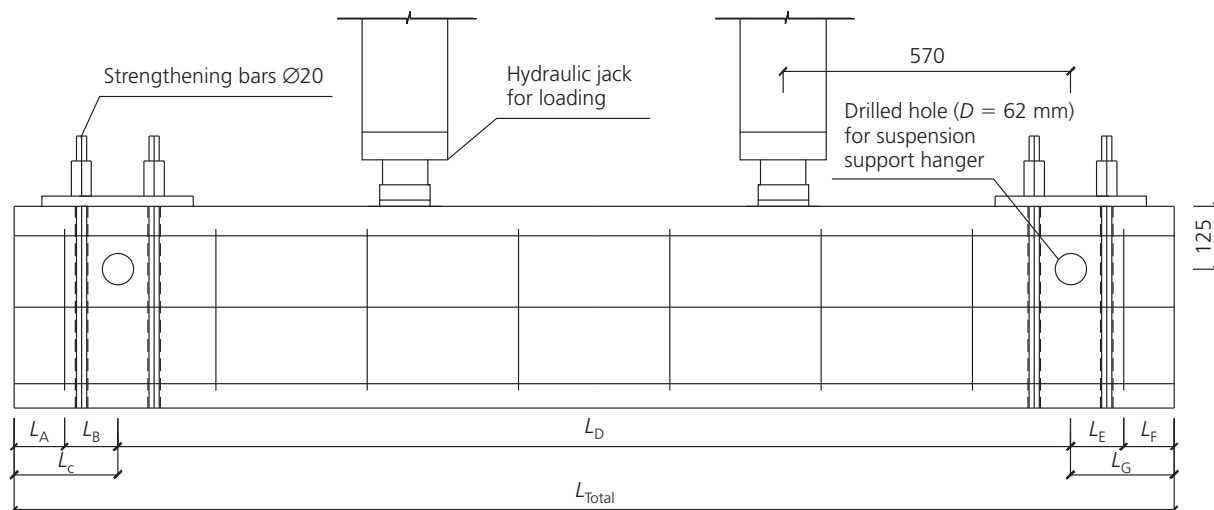the splitting cracks, measured on the sides that later failed, varied

Magazine of Concrete Research
Volume 66 Issue 14

**Anchorage of naturally corroded bars in
reinforced concrete structures**
Tahershamsi, Zandi, Lundgren and Plos

Figure 3. Symmetrical test setup showing the test specimen,
loading jacks and holes for suspension support (dimensions in
mm)

Specimen	L_A: mm	L_B: mm	L_C: mm	L_D: mm	L_E: mm	L_F: mm	L_G: mm	L_{Total}: mm
R4	80	125	205	1870	110	95	205	2280
R6	140	110	250	1815	185	65	250	2315
M4	105	100	205	1875	165	40	250	2285
M5	139	86	225	1882	129	96	225	2332
M7	110	95	205	1893	120	85	205	2303
M8	95	135	230	1840	130	100	230	2300
M9	85	120	205	1878	110	95	205	2288
M10	115	100	215	1860	135	80	215	2290
M11	100	95	195	1886	85	110	195	2276
M12	110	95	205	1885	110	95	205	2295
H5	80	125	205	1890	115	90	205	2300
H6	130	110	240	1800	190	50	240	2280
H7	100	130	230	1855	105	125	230	2315

Table 4. Measured dimensions of the test specimens (see
Figure 3)

from 0·1 mm to 1·5 mm (see Table 5 and Figure 2). Some
examples of the damaged specimens are shown in Figure 4.

General behaviour of the test specimens

In total, thirteen specimens were tested. The specimens showed
similar behaviour concerning crack propagation and failure mode,
while the stiffness and maximum loads varied slightly. Splitting-
induced pull-out was the failure mode in all tested specimens.
Figure 5 shows an example of the results for one of the test
specimens, M4. In these tests, the first flexural cracks were
observed at around 65–95 kN. At this load level, some cracks
propagated around the suspension holes. As the load was in-
creased, some flexural-shear cracks grew over the shear span. The

first inclined shear crack was observed at around 135–155 kN
(see Table 6). As the load increased, the anchorage zones
gradually became loaded. The bond between the reinforcement
and the concrete activated and the free end of the reinforcement
bars started to slip at load levels of 200–220 kN. At this load
level, a second shear crack was observed in some test specimens.
When failure was approaching, splitting cracks occurred on the
side of the beam that later failed in the anchorage zone around
the main bars. However, in specimens H5 and M10, a few
splitting cracks also propagated on the side of the beam that did
not fail. Final anchorage failures occurred on average at load
levels of 281 kN, 267 kN and 266 kN for R, M and H specimens
respectively (Table 7).

Magazine of Concrete Research
Volume 66 Issue 14

Anchorage of naturally corroded bars in
reinforced concrete structures
Tahershamsi, Zandi, Lundgren and Plos

Specimen	Crack width: mm		
	a	b	c
R4	—	—	—
R6	—	—	—
M4	Damaged [a]	Damaged [a]	—
M5	0·6	0·2	—
M7	1·5	—	0·2
M8	0·7	—	—
M9	—	—	—
M10	1·4	—	—
M11	0·9	—	—
M12	1·5	0·1	—
H5	1·5	—	—
H6	Spalling	Spalling	—
H7	Spalling	Spalling	—

[a] Spalling of concrete cover occurred in preparation stage.

Table 5. Observed crack width in the anchorage zone before testing, on the side of the specimen that failed in tests (see Figure 2)

The two R specimens showed rather different results. Photographs of some of the tested beams are shown in Figure 6. During the preparation stage, specimens M4 and M8 were slightly damaged and the concrete cover was spalled at one corner (Figure 4). Therefore, these specimens were regrouped into the H category. However, in M8, anchorage failure occurred on the side with no cover spalling. As mentioned earlier, in specimen M10, splitting cracks propagated on two sides. On the side where the splitting cracks first occurred, one of the bundled bars at one corner started to slip and, later, anchorage failure occurred on the other side. For the H specimens, beams H6 and H7 failed on the side with cover spalling, while failure occurred on the side with the splitting cracks in specimen H5. In specimen R4, rather large deflection was observed in the initial loading stage (Figure 7(a)). This behaviour could be partly related to existing damage due to freezing of the specimen. Zandi Hanjari et al. (2013) explained the phenomenon as the soft behaviour of damaged concrete in the compression zone, which might result in large mid-span deflections.

Available anchorage length

In four-point bending tests, flexural and shear cracks occur in the shear span with an increase of load. After the occurrence of inclined cracks, the tensile force in the reinforcement in the shear span increases. This tensile force in the reinforcement must be transferred to the concrete by bond stresses, and this is called the anchorage (Magnusson, 2000). Based on this definition, the available anchorage length was measured from the crack patterns that appeared after the tests: it was measured from the point where the inclined shear crack met the tensile reinforcement bars

to the end cross-section (see examples in Figure 8). Measurements were taken on the sides of the beam that failed, both rear and front sides. The average anchorage lengths for rear and front sides are listed in Table 8. As can be seen, the values vary from about 250 mm to 500 mm. The available anchorage length showed a lower average value for the R specimens than for the M and H beams. As discussed earlier, for some of the beams, it was necessary to move the support holes closer to the centre in order not to damage the stirrups (Table 4). However, these small variations in geometry did not seem to influence the available anchorage length.

Calculation of average bond stress

The average bond stress along the bundled bars was estimated as follows. The axial force in the longitudinal reinforcement bars was calculated assuming that no tensile force was transferred over the main shear crack (see Figure 9). The inner lever arm was assumed to be $0·9d$, in which the effective height d was taken as the distance between the top of the cross-section to the average position of the tensile reinforcement bars. From equilibrium, the tensile force in the longitudinal reinforcement was thus calculated as
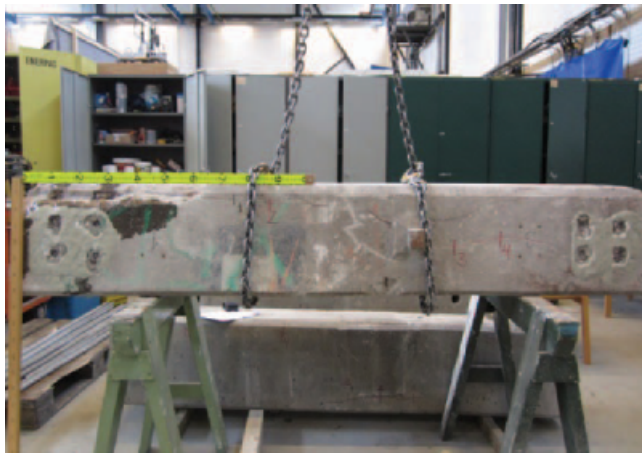
$$1. \qquad F_t = \frac{Pl_s}{0·9d}$$

where P represents the point load and l_s the shear span, which was 570 mm in all the tests. The average bond stress along the bundled bars was then calculated based on the tensile force P, the available anchorage length l_a and the circumference of the bundled bars. For the circumference of two bundled bars, Jirsa et al. (1995) used an upper and lower limit of $\phi 2\pi$ and $\phi(\pi + 2)$ respectively. In this study, the average value of this upper and lower limit was chosen. Since there were two bundles of two bars each, the average bond stress was calculated as
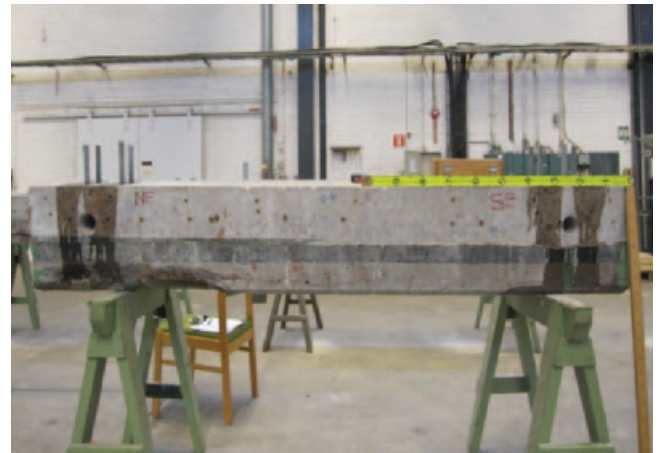
$$2. \qquad \hat{\tau} = \frac{F_t}{l_a(3\pi + 2)\phi}$$

where l_a is the available anchorage length, evaluated as described earlier. More details concerning the calculations are given by Lundgren et al. (2014). The maximum average bond stress of all tests is given in Table 9. The highest bond stress was found in the undamaged specimens. Compared with the R specimens, the M specimens had almost 17% lower maximum bond stress and the H specimens showed a 13% decrease.

Figures 7, 10 and 11 show the calculated average bond stress versus measured average free-end slip for R, M and H specimens respectively (measurement noises were filtered out). It should be noted that the measured slips were all negative for the first test series (Lundgren et al., 2014) and also for the first test in this series (M5) (see Figure 10). The problem was solved in the other tests of this series by measuring the deformation of the concrete

Magazine of Concrete Research
Volume 66 Issue 14

**Anchorage of naturally corroded bars in
reinforced concrete structures**
Tahershamsi, Zandi, Lundgren and Plos

(a) M4

(b) M8

(c) H5 (spalled concrete cover)

(d) M12

Figure 4. Examples of documentation of damage before testing:
(a) M4; (b) M8 (concrete cover spalled in one corner during the
preparation stage); (c) H5 with severe concrete cover spalling,
which failed on the side with only splitting cracks; (d) M12 with a
continuous splitting crack along the failure side

cross-section close to the main bars, as mentioned earlier in the
paper. For these tests, the slip values were corrected by these
measurements. The results clearly showed the initiation points as
well as the magnitudes and rates of the increasing slips. As can
be seen in Figure 7, for the R specimens, the average end slip
started increasing at load levels higher than the initial shear
cracks and rather close to the maximum failure load, around 90%
of the maximum load. For the M specimens, the free-end slip
started at about 75–95% of the maximum load and the slip
values increased up to 0·1–0·8 mm in different tests (Figure 10).
In specimens H6 and H7, the post-peak behaviour was more
stable and the slip values increased up to 2·5 mm. For specimen
H5, in which failure occurred on the side without cover spalling,
the anchorage of the main bars failed in a more brittle manner
(Figure 11). A comparison of beams within each category
revealed that the specimens with relatively lower stiffness in the
load–deformation graphs had a more stable increase of slip
reaching a maximum load and, furthermore, they showed slightly
larger slips at post-peak behaviour. For example, in Figure 7, R4
showed larger deflections for the applied load compared with R6
and the main tensile reinforcements in R4 also showed more
ductile bond behaviour. A residual bond capacity of around 50–
70% of the maximum bond capacity was observed for large slip
values in most of the tests.

Discussion

In total, 21 specimens with differing degrees of corrosion damage
were tested in the first test series (Lundgren *et al.*, 2014) and the
second test series. In both series, the damaged specimens showed
around 5–10% lower load-carrying capacity than the undamaged
ones – 10% for the first test series and 5% for the second. The
average bond stress in the anchorage zone was about 16–17%
lower in the beams with corrosion cracks compared with the R
specimens, and 9–13% lower in the beams with cover spalling. It
should also be noted that the concrete compressive strength f_c of
the damaged specimens was slightly lower than that of the R

Magazine of Concrete Research
Volume 66 Issue 14

Anchorage of naturally corroded bars in
reinforced concrete structures
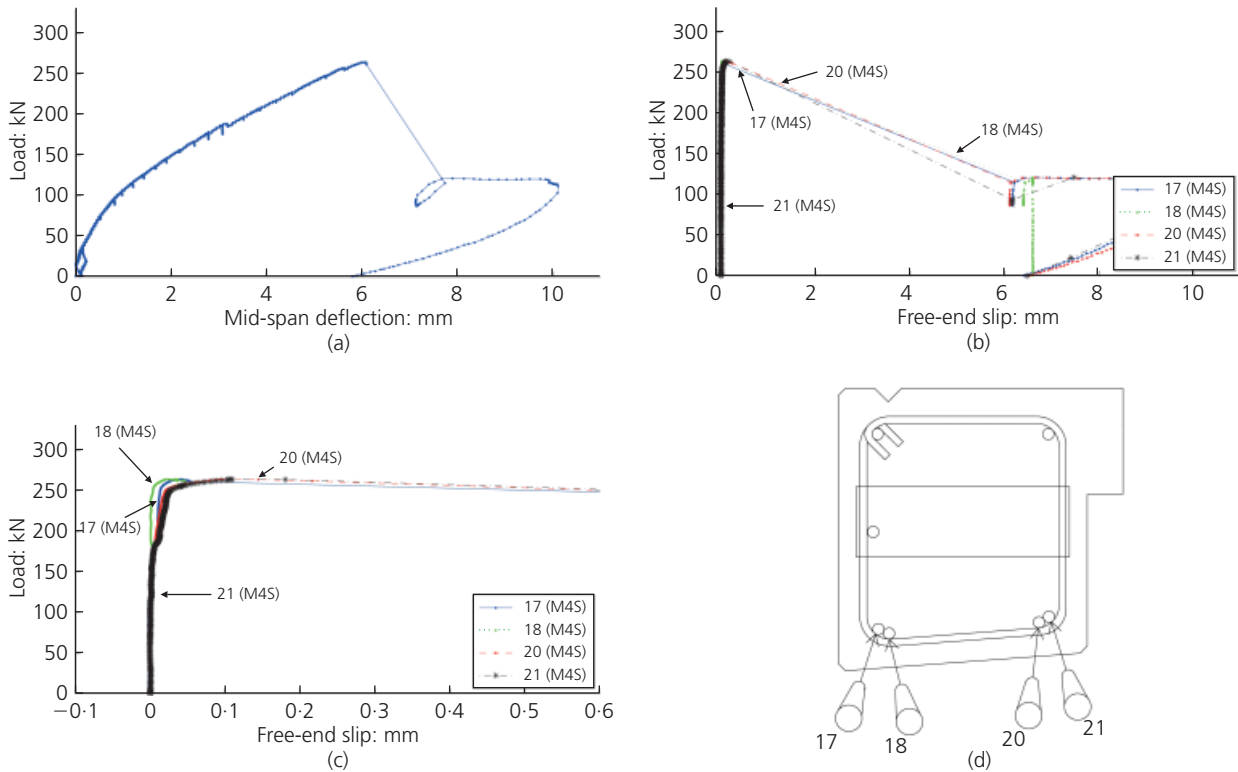Tahershamsi, Zandi, Lundgren and Plos

Figure 5. Test M4: (a) average load from hydraulic jacks versus measured deflection at mid-span (vertical mid-span displacement corrected for the support settlements); (b) average load from hydraulic jacks versus measured slips in each of the bundled bars; (c) enlarged part of Figure 5(b); (d) locations of the measuring transducers. M4S, south side of bar M4

	Beam								
	4	5	6	7	8	9	10	11	12
R	125–155	—	160–170	—	—	—	—	—	—
M	155–185	140–175	—	155–185	155–175	120–173	145–155	155–170	145–155
H	—	135–155	135–145	125–145	—	—	—	—	—

Table 6. Load level (in kN) corresponding to the initial inclined shear cracks observed during the tests; the load values are the average of the load from each of the two hydraulic jacks

	Beam									Average	Standard deviation
	4	5	6	7	8	9	10	11	12		
R	240·1	—	322·0	—	—	—	—	—	—	281·1	57·9
M	263·0	280·9	—	243·3	326·8	234·2	264·9	263·2	259·9	267·0	28·0
H	—	307·6	234·9	255·3	—	—	—	—	—	265·9	37·5

Table 7. Maximum failure load (in kN) obtained in the experiments; the load values are the average of the load from each of the two hydraulic jacks
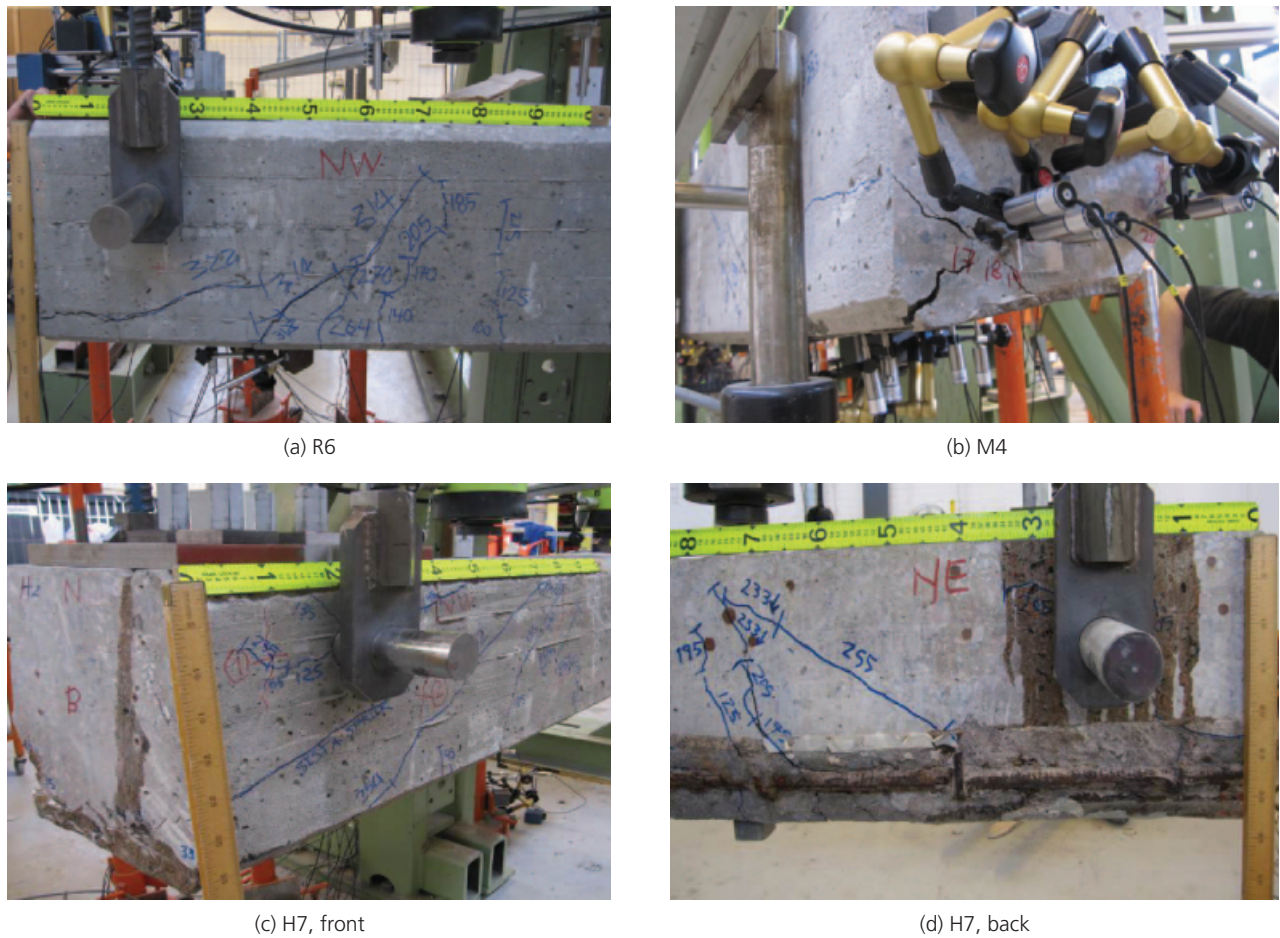
Magazine of Concrete Research
Volume 66 Issue 14

Anchorage of naturally corroded bars in
reinforced concrete structures
Tahershamsi, Zandi, Lundgren and Plos

(a) R6

(b) M4

(c) H7, front

(d) H7, back

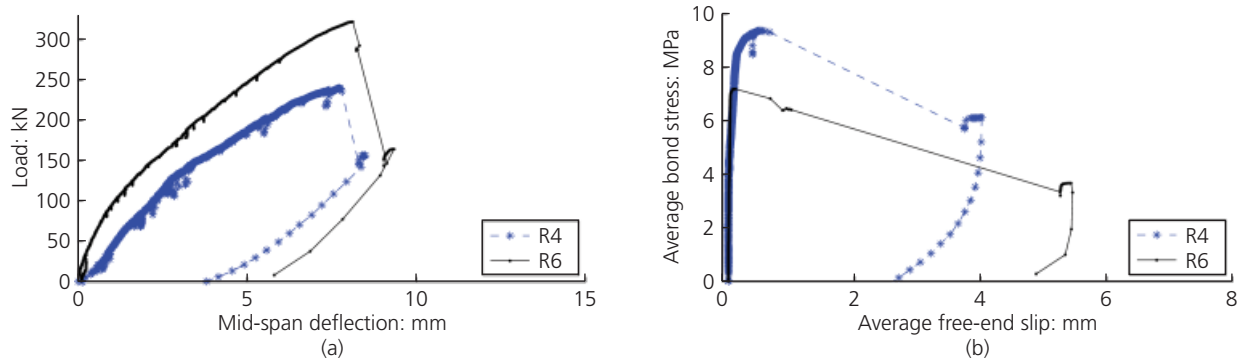**Figure 6.** Failure and crack pattern of some of the beams after
testing

Figure 7. (a) Average load from hydraulic jacks versus measured
deflection at mid span. (b) Average bond stress versus average
measured free-end slip for R specimens

specimens; the samples from damaged specimens showed a 10–
15% reduction in strength.

In the M specimens, it was observed that anchorage failure
occurred on the side where the widest splitting crack was located.

The maximum observed crack widths before structural testing
were measured in the shear and anchorage zones in each speci-
men (Table 10). These values are plotted against the maximum
average bond stress normalised using the average value of the R
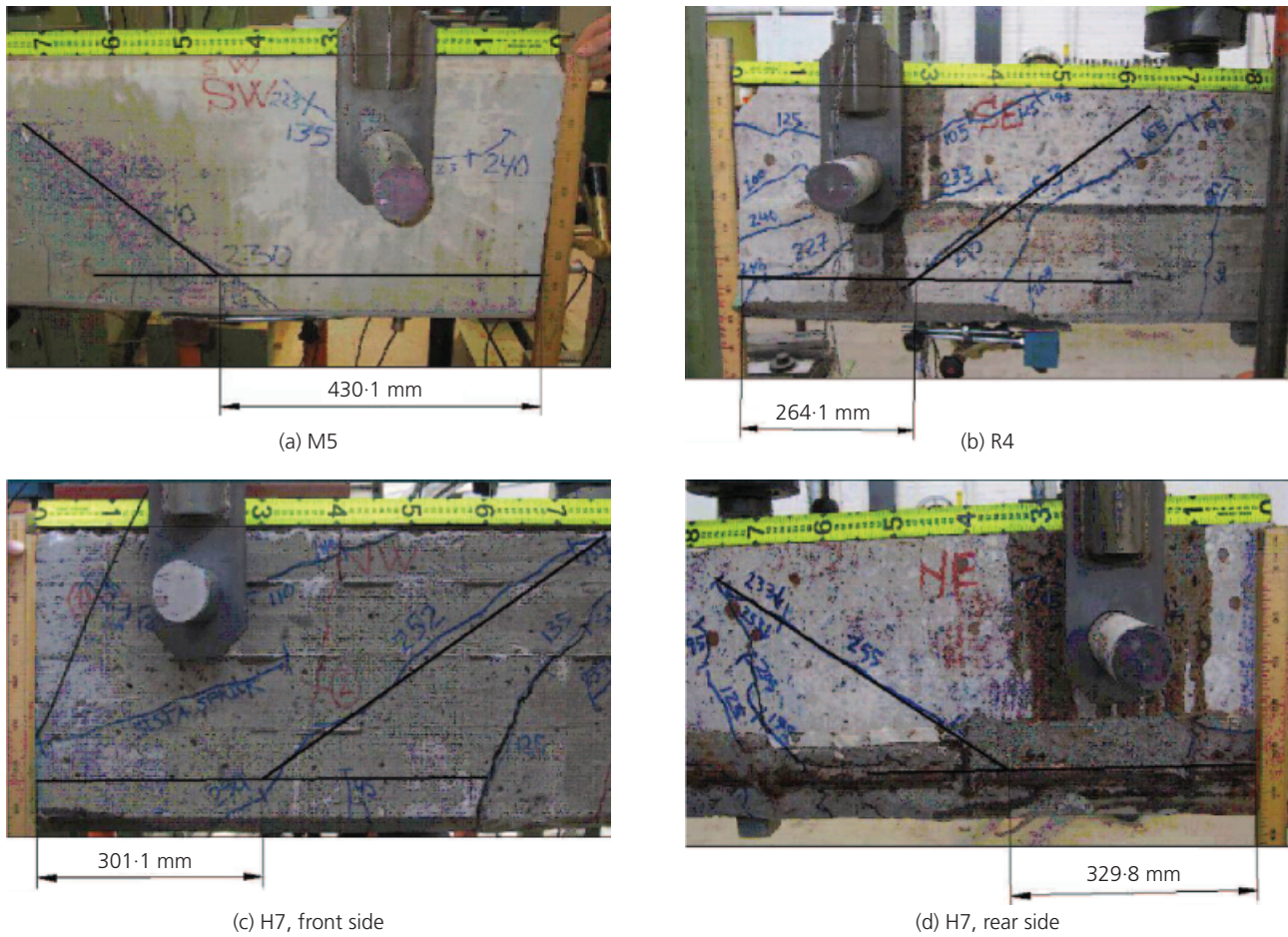specimen in Figure 12. The results indicate decreasing bond

Magazine of Concrete Research
Volume 66 Issue 14

**Anchorage of naturally corroded bars in
reinforced concrete structures**
Tahershamsi, Zandi, Lundgren and Plos

(a) M5

430·1 mm

(b) R4

264·1 mm

(c) H7, front side

301·1 mm

(d) H7, rear side

329·8 mm

Figure 8. Available anchorage length in some of the beams,
measured from the end cross-section to the point where the
main bars and the inclined shear crack intersect

	Beam									Average	Standard deviation
	4	5	6	7	8	9	10	11	12		
R	257	—	437	—	—	—	—	—	—	347	127
M	426	431	—	314	341	337	334	507	501	399	78
H	—	475	427	315	—	—	—	—	—	406	82

Table 8. Available anchorage lengths in the experiments (in mm);
the given values for each specimen are the average of the
measured anchorage length on both edges of the failure zone

capacity with increasing crack width. Model Code 2010 (fib,
2010) suggests a reduction in residual bond strength depending
on the crack width and this is plotted for comparison in Figure
12. As Model Code 2010 gives a range for both bond strength
and crack width, it was decided to plot the interval as the ranges
in bond strength versus the average values of the relevant crack
width ranges. As the figure shows, the upper and lower limits for

the residual bond strength also have a descending trend with
respect to the increase in crack width. It can be observed that the
residual bond capacities of the naturally corroded specimens were
higher than the upper limit in Model Code 2010.

Furthermore, in Figure 12, the results of the present study are
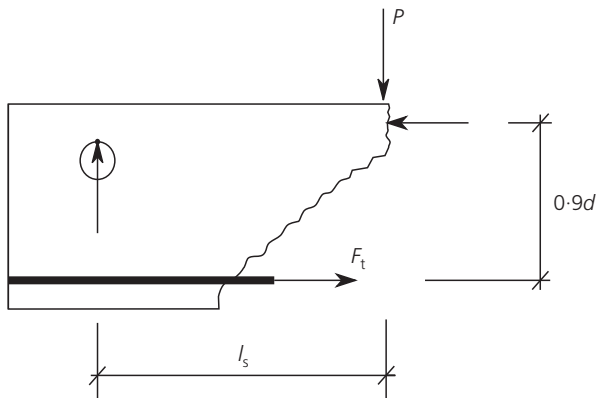compared with two different test series of accelerated corroded

Magazine of Concrete Research
Volume 66 Issue 14

Anchorage of naturally corroded bars in
reinforced concrete structures
Tahershamsi, Zandi, Lundgren and Plos

Figure 9. Notation used in estimation of the tensile force in the longitudinal reinforcement

specimens carried out by Rodriguez *et al.* (1994) and Zandi Hanjari and Coronelli (2010). The results from the naturally corroded specimens in this study and the artificially corroded tests are different. The bond strength of the naturally corroded bars was considerably higher than that of the artificially corroded specimens. It is worth mentioning that the range of measured crack widths in the naturally corroded samples was wider than with the artificially corroded specimens in the previous studies. Andrade and Alonso (1993) found that crack width depended not only on the corrosion level (reduction of bar cross-sectional area) but also on the applied current density (corrosion rate). For the same corrosion level and with low corrosion rates, larger crack widths appeared on the concrete surface.

As expected, the maximum average bond stress depends on the available anchorage length (Figure 13). The measured available anchorage length varied between 250 and 500 mm in the present study while it was fixed to a value of 210 mm in both the accelerated corrosion studies mentioned earlier. Furthermore, the artificially corroded specimens had a greater number of stirrups. It is therefore noteworthy that, for the same crack width, in spite of these differences, higher bond stresses were obtained in the naturally corroded tests than in the artificially corroded specimens.

Calculation of the stress in transverse and longitudinal reinforcements indicated that no yielding occurred until failure (Berg and

Johansson, 2011). To evaluate the amount of transverse reinforcement, a comparison was made with the provisions given in Eurocode 2 (CEN, 2004). The code requires that the area of transverse reinforcement in the anchorage zone is larger than 25% of the largest anchored bar or else the amount of transverse reinforcement will not be sufficient to contribute to the anchorage. In the tested specimens, there was only one stirrup with a bar diameter of 10 mm within the available anchorage length. This means that the area of the transverse reinforcement in the anchorage zone was only 19·5% of the largest anchored bar. Therefore, according to Eurocode 2, the amount of transverse reinforcement is not sufficient to have an influence on the anchorage capacity.

Corrosion measurements

In the first test series, some specimens were broken and the tensile reinforcements removed. The bars were thoroughly cleaned in accordance with ASTM G1-03. The reinforcement bars removed from the damaged specimens showed severe pitting corrosion. The corrosion level was measured using a weight loss method. The weight loss in the corroded specimens was about 2–3% compared with that of an uncorroded specimen. In comparison with the tested reference bar, the yield strength of the corroded bars was reduced by 0·5–20·0%, and the ultimate strength by 4–26%. The ductility of the corroded bars was significantly reduced. For further details on these results, see Lundgren *et al.* (2014). In the second test series, all the broken specimens were saved for more accurate measurements of the corrosion level.

Conclusion and outlook

Thirteen specimens with varying degrees of natural corrosion were tested in an indirectly supported four-point bending test. In all the experiments, splitting-induced pull-out failure occurred after the appearance of diagonal shear cracks. Compared with undamaged reference specimens, the specimens with medium and high levels of damage had approximately 5% lower load-carrying capacity. The maximum capacities in the reference beams showed a larger scatter. Specimens with relatively lower bending stiffness showed a more ductile bond failure. The available anchorage lengths were measured after the tests, between the intersection point of the main inclined shear crack and the tensile bars to the end cross-section; they varied from 250 to 500 mm. The average

	Beam									Average	Standard deviation
	4	5	6	7	8	9	10	11	12		
R	9·4	—	7·2	—	—	—	—	—	—	8·3	1·5
M	6·2	6·6	—	7·9	9·3	6·9	8·0	5·2	5·2	6·9	1·4
H	—	6·9	6·0	8·7	—	—	—	—	—	7·2	1·4

Table 9. Maximum average bond stress (in MPa) in the experiments

Magazine of Concrete Research
Volume 66 Issue 14

Anchorage of naturally corroded bars in
reinforced concrete structures
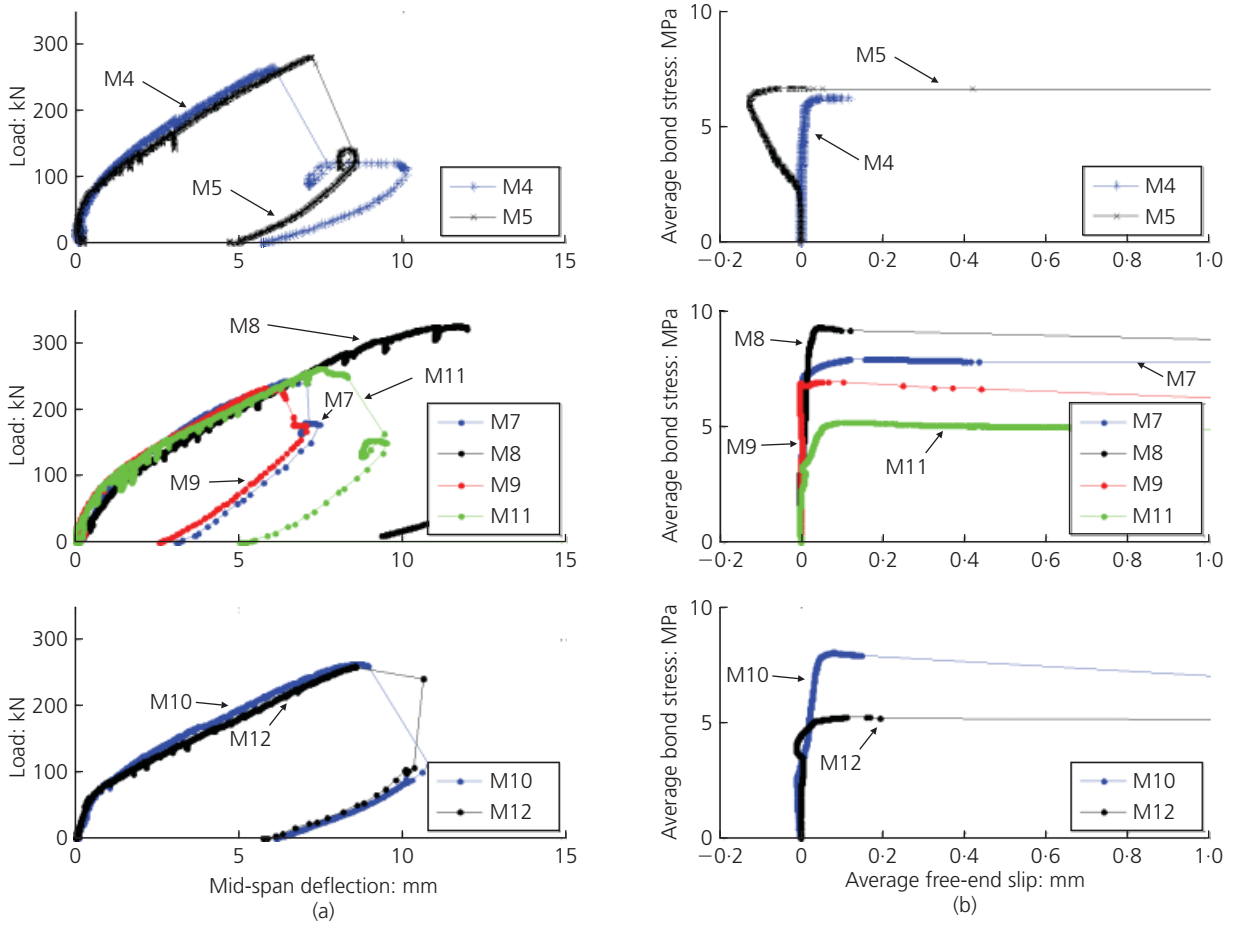Tahershamsi, Zandi, Lundgren and Plos

Figure 10. (a) Average load from hydraulic jacks versus measured
deflection at mid-span. (b) Average bond stress versus average
measured free-end slip for M specimens. The specimens were
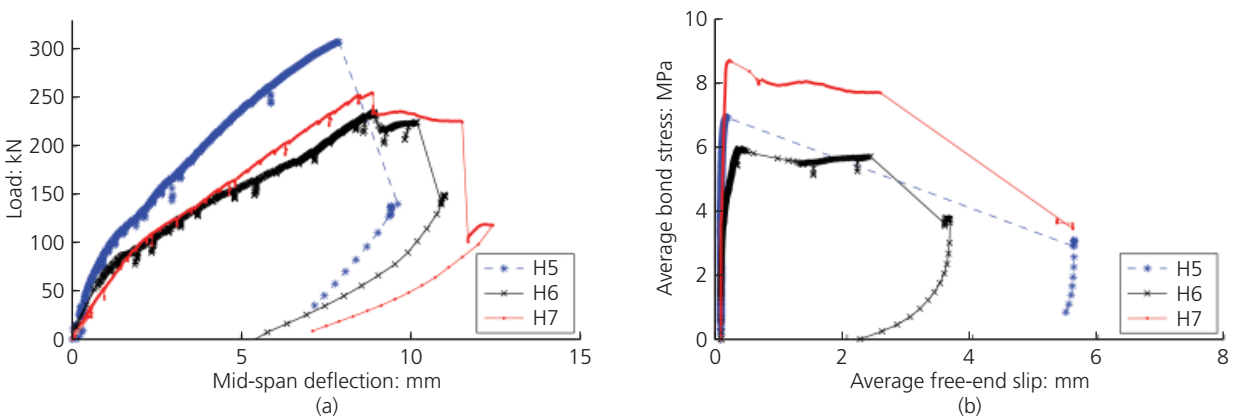categorised into three groups regarding their bending stiffness

Figure 11. (a) Average load from hydraulic jacks versus measured
deflection at mid-span. (b) Average bond stress versus average
measured free-end slip for H specimens

Stiffness	Specimen	Failure side	Minimum crack width: mm	Maximum crack width: mm	Crack pattern			Maximum failure load: kN	Bond stress: MPa	Available anchorage length: mm
					Bottom	Front	Rear			
	R4	L	—	—				240·1	9·4	257
	R6	R	—	—				322·0	7·2	437
Highest	M4	L	0·1	2·5				263·0	6·2	426
	M5	L	0·1	0·6				280·9	6·6	431
Medium	M7	R	0·1	1·5				243·3	7·9	314
	M8	R	0·1	0·7				326·8	9·3	341
	M9	L	0·1	2·0				243·2	6·9	337
	M11	L	0·1	2·2				263·2	5·2	507
Lowest	M10	R	0·1	1·4				264·9	8·0	334
	M12	R	0·1	2·0				259·9	5·2	501

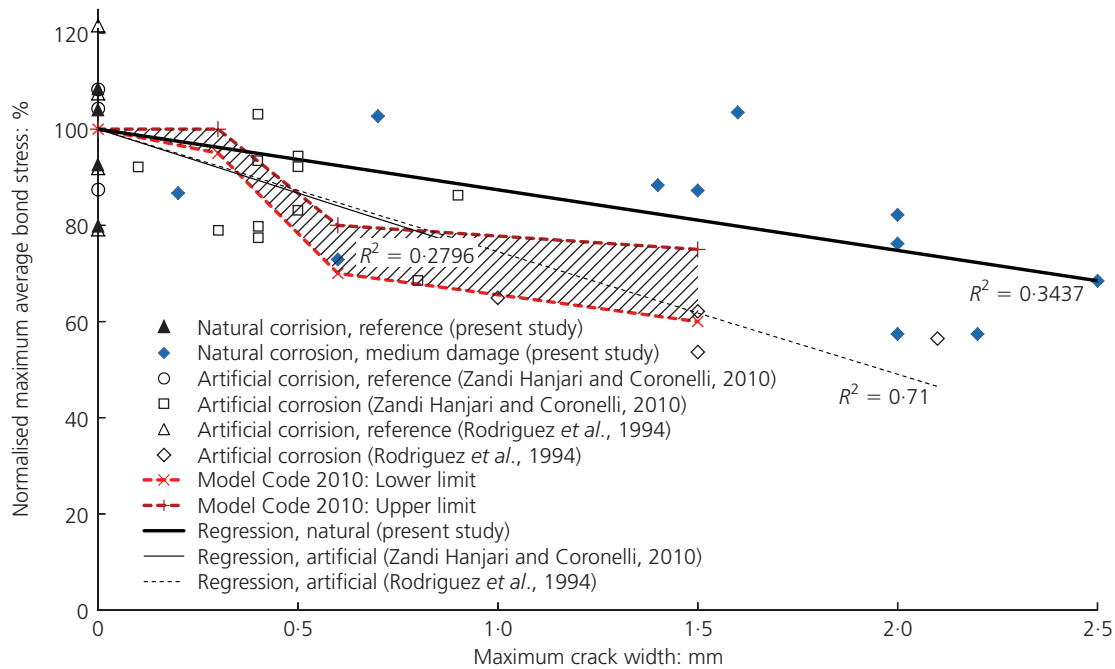**Table 10.** Crack pattern and width documentation along with summary of test results for R and M specimens

Figure 12. Comparison of test results from naturally corroded specimens with artificially corroded tests and with Model Code 2010 in terms of bond strength, normalised with respect to the average maximum bond strength obtained from R samples, versus maximum crack width
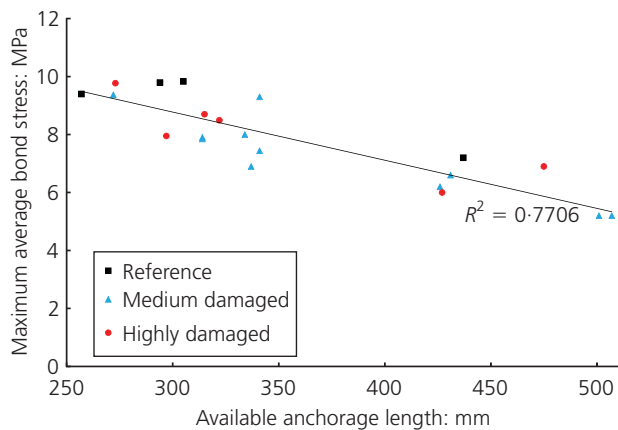

Figure 13. Maximum average bond stress in the anchorage zone versus the measured available anchorage length

bond stress in the anchorage area was calculated from the applied load and the available anchorage length. The values obtained showed a 17% reduction in average bond stress in specimens with cover cracking only (medium damage) and 13% for the beams with cover spalling (high damage) compared with the reference beams. Material tests on the concrete showed a 10–15% strength reduction in compressive strength of the damaged specimens. Comparison of the results from artificial and natural corrosion showed both similarities and differences in the mechanical behaviour of reinforced concrete members. In both accelerated and natural corrosion, a reduction in residual bond strength was

observed for increased maximum measured crack widths. Model Code 2010 (fib, 2010) also reports such a trend. However, the residual bond strength in the naturally corroded specimens was considerably higher than both the artificially corroded specimens and the limits given in Model Code 2010.

The tests conducted in this research have produced benchmark data for anchorage behaviour in naturally corroded reinforcements. For a better understanding of the mechanical behaviour of natural corrosion, the test results obtained will be evaluated using a more advanced method than the one used thus far – the new datasets will be analysed with advanced 3D finite-element models utilising the available bond and corrosion models developed by Lundgren (2005) and Zandi Hanjari et al. (2011a). In the work described in this paper, specimens were qualitatively classified through damage observations. Therefore, for detailed study of the corrosion levels, the conventional methods of weight loss should be complemented with more advanced volumetric 3D scanning measurements. The results from the two test series reported here and elsewhere (Lundgren et al., 2014) have yielded valuable information on the anchorage behaviour in naturally corroded concrete structures. However, considering that the results differ from artificially corroded specimens, more tests on naturally corroded structures are still needed.

Acknowledgements

Magazine of Concrete Research
Volume 66 Issue 14

Anchorage of naturally corroded bars in
reinforced concrete structures
Tahershamsi, Zandi, Lundgren and Plos

REFERENCES

Almusallam AA (2001) Effect of degree of corrosion on the
properties of reinforcing steel bars. *Construction and
Building Materials* **15(8)**: 361–368.

Al-Sulaimani GJ, Kaleemullah M, Basunbul IA *et al.* (1990)
Influence of corrosion and cracking on bond behavior and
strength of reinforced concrete members. *ACI Structural
Journal* **87(2)**: 220–231.

Andrade C and Alonso C (1993) Cover cracking as a function of
bar corrosion: part I – experimental test. *Materials and
Structures* **26(8)**: 453–464.

ASTM (2003) ASTM:GI-03: Standard practice for preparing,
cleaning and evaluating corrosion test specimens. ASTM
International, West Conshohocken, PA, USA.

Austin SA, Lyons R and Ing MJ (2004) Electrochemical behavior
of steel-reinforced concrete during accelerated corrosion
testing. *Corrosion* **60(2)**: 203–212.

Berg F and Johansson D (2011) *Design of Test Set-up Using FEM
Pilot Tests on Anchorage of Naturally Corroded
Reinforcement*. Chalmers University of Technology,
Gothenburg, Sweden.

BSI (2009a) BS EN 12504-1: 2009 Testing concrete in structures.
Cored specimens. Taking, examining and testing in
compression. BSI, London, UK.

BSI (2009b) BS EN 12390-3: 2009 Testing hardened concrete.
Compressive strength of test specimens. BSI, London, UK.

CEN (Comité Européen de Normalisation) (2004) Eurocode 2:
Design of concrete structures. Part 1: general rules and rules
for buildings. CEN, Brussels, Belgium.

Coronelli D (1997) Bond of corroded bars in confined concrete:
test results and mechanical modelling. *Studi e Ricerche della
Scuola di Specializzaziona in Costruzioni in c. a. Politecnico
di Milano* **18**: 137–211.

Coronelli D and Gambarova P (2004) Structural assessment of
corroded reinforced concrete beams: modeling guidelines.
Journal of Structural Engineering **130(8)**: 1214–1224.

Coronelli D, Hanjari KZ and Lundgren K (2013) Severely
corroded RC with cover cracking. *Journal of Structural
Engineering* **139(2)**: 221–232.

Du YG, Clark LA and Chan AHC (2005a) Effect of corrosion on
ductility of reinforcing bars. *Magazine of Concrete Research*
57(7): 407–419.

Du YG, Clark LA and Chan AHC (2005b) Residual capacity of
corroded reinforcing bars. *Magazine of Concrete Research*
57(3): 135–147.

fib (International Federation for Structural Concrete) (2010)
Model Code 2010, Vol. 1. fib, Lausanne, Switzerland.

Gestsdottir E and Gudmundsson T (2012) *Bond Behaviour of
Naturally Corroded Reinforcement in Concrete Structures*.
Chalmers University of Technology, Gothenburg, Sweden.

Jirsa JO, Chen W, Grant DB and Elizondo R (1995) *Development
of Bundled Reinforcing Steel*. The University of Texas at
Austin, Austin, TX, USA.

Lundgren K (2005) bond between ribbed bars and concrete. Part
2: The effect of corrosion. *Magazine of Concrete Research*
57(7): 383–395.

Lundgren K, Tahershamsi M, Zandi Hanjari K and Plos M (2014)
Tests on anchorage of naturally corroded reinforcement in
concrete. *Journal of Materials and Structures*. Published
online. See http://link.springer.com/article/10.1617/s11527-
014-0290-y (accessed 15/05/2014).

Magnusson J (2000) *Bond and Anchorage of Ribbed Bars in
High-Strength Concrete*. Chalmers University of Technology,
Gothenburg, Sweden.

Regan PE and Kennedy Reid IL (2010) *Assessment of Concrete
Structures Affected by Delamination – 2*. Graduate School in
Concrete Structures, Politecnico di Milano, Milan, Italy.

Rodriguez J, Ortega LM and Garda AM (1994) Assessment of
structural elements with corroded reinforcement. In
*Proceedings of International Conference on Corrosion and
Corrosion Protection of Steel in Concrete, Sheffield, UK*
(Swamy RN (ed.)). Sheffield Academic Press Ltd., Sheffield,
UK pp. 171–185.

Sæther I (2011) Bond deterioration of corroded steel bars in
concrete. *Structure and Infrastructure Engineering* **7(6)**: 415–
429.

Saifullah M and Clark LA (1994) Effect of corrosion rate on the
bond strength of corroded reinforcement. In *Proceedings of
International Conference on Corrosion and Corrosion
Protection of Steel in Concrete, Sheffield, UK* (Swamy RN
(ed.)). Sheffield Academic Press Ltd., Sheffield, UK, pp.
591–602.

Tahershamsi M, Zandi Hanjari K, Lundgren K and Plos M (2012a)
Anchorage capacity of naturally corroded reinforced concrete
beams. In *Proceedings of fib Symposium on Concrete
Structures for Sustainable Community* (Bager DH and
Silfwerbrand J (eds)). fib, Stockholm, Sweden, pp. 323–326.

Tahershamsi M, Zandi Hanjari K, Lundgren K and Plos M (2012b)
Anchorage in naturally corroded specimens taken from
existing structures. In *Bond in Concrete 2012: Bond,
Anchorage, Detailing. Fourth International Symposium,
Volume 1: General Aspects of Bond* (Cairns JW, Metelli G and
Plizzari GA (eds)). Manerbio, Brescia, Italy, pp. 345–349.

Val DV, Chernin L and Stewart MG (2009) Experimental and
numerical investigation of corrosion-induced cover cracking
in reinforced concrete structures. *Journal of Structural
Engineering* **135(4)**: 376–385.

Yuan Y, Ji Y and Shah SP (2007) Comparison of two accelerated
corrosion techniques for concrete structures. *ACI Structural
Journal* **104(3)**: 344–347.

Zandi Hanjari K and Coronelli D (2010) *Anchorage Capacity of
Corroded Reinforcement. Eccentric Pull-out Tests*. Chalmers
University of Technology, Gothenburg, Sweden.

Zandi Hanjari K, Coronelli D and Lundgren K (2011a) Bond
capacity of severely corroded bars with corroded stirrups.
Magazine of Concrete Research **63(12)**: 953–968.

Zandi Hanjari K, Kettil P and Lundgren K (2011b) Analysis of mechanical behavior of corroded reinforced concrete structures. *ACI Structural Journal* **108(5)**: 532–541.

Zandi Hanjari K, Kettil P and Lundgren K (2013) Modelling the structural behaviour of frost-damaged reinforced concrete structures. *Structure and Infrastructure Engineering* **9(5)**: 416–431.